Dynamics of Atmospheres and Oceans 49 (2010) 25–36

Contents lists available at ScienceDirect

Dynamics of Atmospheres and Oceans

journal homepage: www.elsevier.com/locate/dynatmoce

# Mixing efficiency in decaying stably stratified turbulence

Derek D. Stretch[a], James W. Rottman[b,*], S.Karan Venayagamoorthy[a,1], Keiko K. Nomura[b], Chris R. Rehmann[c]

[a] School of Civil Engineering, University of KwaZulu-Natal, Centenary Building, King George V Avenue, Durban 4041, South Africa
[b] Department of Mechanical and Aerospace Engineering, University of California, San Diego, 9500 Gilman Drive, La Jolla, CA 92093-0402, USA
[c] Department of Civil, Construction, & Environmental Engineering, Iowa State University, 374 Town Engineering, Ames, IA 50011, USA

ARTICLE INFO

*Article history:*
Received 21 August 2007
Received in revised form 2 November 2008
Accepted 4 November 2008
Available online 13 November 2008

*Keywords:*
Turbulence
Stable stratification
Mixing efficiency

ABSTRACT

Mixing efficiency in stratified flows is a measure of the proportion of turbulent kinetic energy that goes into increasing the potential energy of the fluid by irreversible mixing. In this research direct numerical simulations (DNS) and rapid distortion theory (RDT) calculations of transient turbulent mixing events are carried out in order to study this aspect of mixing. In particular, DNS and RDT of decaying, homogeneous, stably-stratified turbulence are used to determine the mixing efficiency as a function of the initial turbulence Richardson number $Ri_{t0} = (NL_0/u_0)^2$, where $N$ is the buoyancy frequency and $L_0$ and $u_0$ are initial length and velocity scales of the turbulence. The results show that the mixing efficiency increases with increasing $Ri_{t0}$ for small $Ri_{t0}$, but for larger $Ri_{t0}$ the mixing efficiency becomes approximately constant. These results are compared with data from towed grid experiments. There is qualitative agreement between the DNS results and the available experimental data, but significant quantitative discrepancies. The grid turbulence experiments suggest a maximum mixing efficiency (at large $Ri_{t0}$) of about 6%, while the DNS and RDT results give about 30%. We consider two possible reasons for this discrepancy: Prandtl number effects and non-matching initial conditions. We conclude that the main source of the disagreement probably is due to inaccuracy in determining the initial turbulence energy input in the case of the grid turbulence experiments.



* Corresponding author. Tel.: +1 858 534 7002; fax: +1 858 534 7599.
*E-mail address:* jrottman@ucsd.edu (J.W. Rottman).
[1] Current address: Department of Civil and Environmental Engineering, Colorado State University, 1372 Campus Delivery, Fort Collins, CO 80523-1372, USA.

0377-0265/$ – see front matter © 2008 Elsevier B.V. All rights reserved.
doi:10.1016/j.dynatmoce.2008.11.002

## 1. Introduction

Mixing in stably stratified geophysical flows often occurs during transient episodic events, such as the local breakdown of internal waves or shear instabilities or the motion of fish, where the lack of a sustained source of energy leads to the dissipation of the turbulence associated with these events. The mixing efficiency of such events is a measure of the proportion of initial turbulent kinetic energy that goes into increasing the potential energy of the fluid by irreversible mixing. How this mixing efficiency varies with stratification can be important for understanding and modeling mixing processes in geophysical flows (e.g. Gregg, 1987, 1998; Ivey et al., 2008). More recent interest in this topic has been raised by Dewar et al. (2006) who have proposed that the marine biosphere is as effective as the wind and the tides in mixing the ocean.

The laboratory experiments of Britter (1985), Rottman and Britter (1986), Barrett and Van Atta (1991), Barry et al. (2001) and Rehmann and Koseff (2004) (see also the corrections given in Rehmann and Koseff, 2005) have attempted to measure the mixing efficiency of decaying grid turbulence in uniformly stratified fluids as a function of a bulk Richardson number $Ri_b = (NM/U)^2$, where $N$ is the buoyancy frequency of the fluid, $M$ is the grid mesh length, and $U$ is the grid towing speed. All these experiments were conducted in a water tank using either salt or heat to produce the stratification. The mixing efficiency, or equivalently an integral flux Richardson number $R_f$, is defined in these experiments as the ratio of the change in potential energy of the fluid to the amount of work done towing the grid through the tank. The experimental results are all reasonably consistent, indicating that for $Ri_b < 1$, the mixing efficiency increases with $Ri_b$, but for larger $Ri_b$ approaches a constant value of about 6%. The results of these experiments do not appear to depend strongly on the Prandtl (or Schmidt) number, $Pr$, which is about 700 for salt-stratified experiments and 7 for the heat-stratified experiments. Reynolds numbers for the experiments were in the range $1000 \leq UM/\nu \leq 36,000$. For the range of Reynolds numbers and Richardson numbers used in these experiments, the turbulence is quite active and molecular effects would be expected to be small.

There are two issues arising from these results. Firstly, since none of the laboratory experiments could achieve values of $Ri_b$ much greater than about 10, it is not conclusive whether the mixing efficiency remains constant for larger $Ri$. In the experiments layers were observed to form when $Ri_b > 1$. Some different types of experiments (see, e.g. Linden, 1980) have suggested that $R_f$ should decrease for sufficiently large $Ri_b$. Secondly, the maximum mixing efficiency of 6% is lower than has been measured in other types of mixing experiments where values of 10–20% are more typical, see, e.g. Linden (1979) and Park et al. (1994).

In the work described here, for the first time direct numerical simulations (DNS) of decaying, homogeneous, stably-stratified turbulence are used to address these two issues. Simulations of this flow are not new: previous DNS results have been reported by Riley et al. (1981), Metais and Herring (1989), Kimura and Herring (1996), and Kaneda and Ishida (2000). However, no results concerning the mixing efficiency have been previously reported from these DNS studies. As Gregg (1987) has pointed out in his review of diapycnal mixing in the ocean thermocline, the change in the mean potential energy is what oceanographers most need for interpreting oceanic data. Other DNS studies of stratified flows, but incorporating the effects of shear, have been reported by Caulfield and Peltier (2000), Smyth et al. (2001), Staquet (2000), Staquet and Bouruet-Aubertot (2001). While these studies have reported results for mixing efficiencies, they have not explored the integrated mixing over a transient homogeneous event that is the focus of this paper.

## 2. Laboratory experiments

The experiments of Britter (1985), Rottman and Britter (1986), Barrett and Van Atta (1991) and Rehmann and Koseff (2004) were all conducted by towing a biplanar grid at a constant speed through a uniformly stratified water. The stratification was produced by salinity gradients, except that in some of the experiments of Rehmann and Koseff (2004) the stratification was produced by temperature gradients, and in one case both temperature and salt were used as the stratifying agents. These experiments cover a range of Prandtl (or Schmidt) numbers $5 < Pr < 700$. Before each set of tows the density profile was measured. After each set of tows the tank was allowed to settle, and when the fluid motion

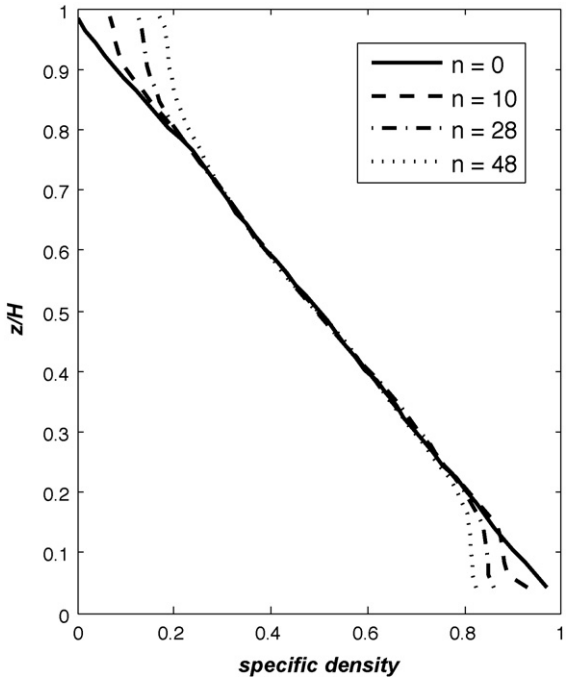


**Fig. 1.** The evolution of the vertical distribution of density after $n = 0$, 10, 28 and 48 grid tows, for the case with $Ri_b = 0.41$, from Rottman and Britter (1986). The vertical coordinate is scaled by the depth of the water in the tank and the density is scaled such that initially it is zero at the top of the tank and unity at the bottom.

was judged to be negligible the vertical density profile was measured again in order to determine the change in the vertical density profile and thus the change in the potential energy of the water in the tank. The measured vertical density profiles for several sets of tows from Rottman and Britter (1986) for the case with $Ri_b = 0.41$ are shown in Fig. 1. The initially linear profile changes by developing well-mixed regions at the top and bottom of the tank with the central portion remaining nearly unchanged. The grid generated turbulence may be thought of as raising the center of mass of the water in the tank by 'diffusing' the heavier/lighter fluid up/down the density gradient. The buoyancy frequency of the central portion of the tank remains remarkably constant until the tank of fluid is almost completely mixed.

In the most strongly stratified cases where the grid Froude number $F = U/MN = Ri_b^{-1/2}$ was less than a critical value of about 1, it was observed that the density profiles in these experiments developed a layered or "staircase" structure, as shown for example in Fig. 3 of Rehmann and Koseff (2004), with vertical scales reflecting the grid spacing. The results for these cases should be treated with caution in the context of the discussion that follows since the initial turbulence generated by the grid is probably not homogeneous and may therefore differ fundamentally from the cases with sub-critical grid Froude numbers. The non-homogeneity is due to the stratification preventing the wakes from the grid from fully merging thus significantly changing the initial conditions for the experiments in those cases.

### 2.1. The energy input

Both Rottman and Britter (1986) and Rehmann and Koseff (2004) measured the mean value of the drag on the grid and deduced the mean value of the drag coefficient, $C_D$, from

$$D = C_D \frac{1}{2} \rho_0 U^2 A \tag{1}$$

where $D$ is the mean drag force from one set of tows, $\rho_0$ is the mean density of the water in the tank, $U$ is the tow speed, and $A$ is the cross-sectional area of the tank occupied by the water.

The total energy $E$ input into the water during each tow is given by

$$E = D\,L_T \tag{2}$$

where $L_T$ is the length of the tank.

### 2.2. The mixing efficiency

The mixing efficiency is defined as the ratio of the change in the potential energy of the fluid in the tank to the total amount of energy input into turbulent motions in towing the grid through the tank. This ratio is a form of integrated flux Richardson number $R_f$. The potential energy $E_{p_n}$ of the water in the tank after $n$ tows is given by

$$E_{p_n} = L_T\,W_T \int_0^H \bar{\rho}_n(z)\,g\,z\,dz \tag{3}$$

where $\bar{\rho}_n$ is the measured density vertical profile after the motion in the tank has subsided after $n$ tows, $W_T$ is the width of the tank and $H$ is the depth of the water. In the analysis of the experimental results by Britter (1985), Rottman and Britter (1986) and Rehmann and Koseff (2004), all the energy input into the water by the towed grid was assumed to go into turbulent motions. Therefore, the integrated flux Richardson number is given by

$$R_{f_n} = \frac{E_{p_n} - E_{p_0}}{n\,E} \tag{4}$$

It was found that $R_{f_n}$ decreased as $n$ increased because the amount of turbulent kinetic energy available for mixing decreased as the well-mixed areas increased in size. A useful measure of the mixing efficiency in which all the turbulent energy is available for mixing is

$$R_f = \lim_{n\to 0} R_{f_n}. \tag{5}$$

Examples of the dependence of $R_{f_n}$ on $n$ are shown in Fig. 2. Also shown in this figure are the least-squares straight line fits to the data that were used to obtain $R_f$ by extrapolation to $n = 0$.

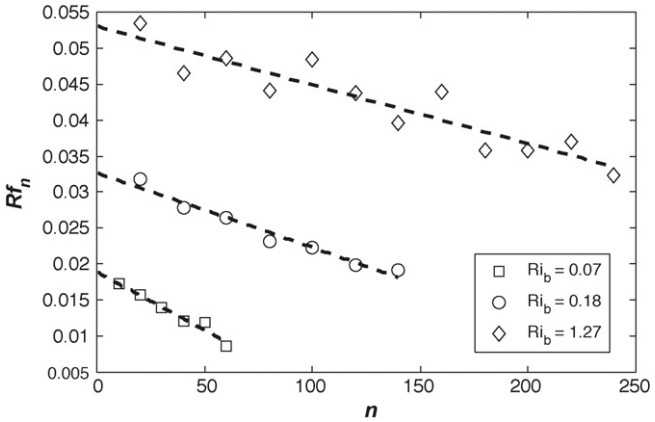


**Fig. 2.** The values of $R_{f_n}$ as a function of $n$ for the cases with $Ri_b = 0.18$, 0.41 and 1.27, from Rottman and Britter (1986). The dashed lines are least-squares straight line fits to these data points.

## 3. Numerical experiments

The numerical experiments were carried out with the pseudo-spectral DNS code described by Riley et al. (1981). The code simulates a flow field that is periodic in all three spatial co-ordinates, with uniform background density gradient.

### 3.1. Initialization

For all our numerical experiments, the turbulent flow field was initialized as a Gaussian, isotropic and solenoidal velocity field in the usual way using random Fourier modes with a specified energy spectrum. The turbulence was then allowed to decay until approximately 99% of the initial turbulence energy had dissipated. Decay times of about ten times the initial time scale of the turbulence $L_0/u_0$ typically were required, where $L_0$ and $u_0$ are the initial length and velocity scales as determined by the specified initial spectrum. The stable stratification for each transient experiment was specified by the initial Richardson number, which was varied in the range $0 < Ri_{t0} < 1000$. The Richardson number for these simulations is defined as $Ri_{t0} = (NL_0/u_0)^2$. With this definition of the Richardson number, the decay time of the turbulence is about $(10/2\pi)\, Ri_{t0}$ buoyancy periods.

The energy spectrum $E(k)$, where $k$ is the wavenumber magnitude, of the initial turbulence was chosen to have the exponential form (see, e.g. Townsend, 1976):

$$E(k) = C\, u_0^2 L_0^5 k^4 \, exp\left(-\frac{1}{2} k^2 L_0^2\right) \tag{6}$$

where $C$ is a constant scaling factor chosen such that

$$\int_0^\infty E(k)\, dk = \frac{3}{2} u_0^2. \tag{7}$$

For most of the simulations, the initial energy was exclusively kinetic in form, i.e., the initial density fluctuations were set to zero. Since one of our main objectives is to compare the simulation results with experimental measurements, the appropriate modeling of the initial conditions is necessary. Experimental measurements downstream of grid generated turbulence in stratified fluids suggest that the *PE* close to the grid (say at $x/M = 10$) is typically only a small fraction of the *KE*, approximately 10% (possibly increasing with increasing stratification). On this basis it seems that the above initialization scheme is a reasonable model for the experiments, although it should be noted that Hunt et al. (1988) have indicated that the flow evolution can be sensitive to the *PE* initial conditions.

### 3.2. Evaluating the mixing efficiency

The energetics of decaying homogeneous, stably stratified turbulence may be described by

$$\frac{d(KE)}{dt} = -b - \epsilon_{KE} \tag{8}$$

$$\frac{d(PE)}{dt} = b - \epsilon_{PE} \tag{9}$$

where $KE = (1/2)(u^2 + v^2 + w^2)$ is the turbulent kinetic energy, $PE = -(1/2)(g/\rho_0)(\partial\bar{\rho}/\partial z)^{-1}\overline{\rho^2}$ is the (available) turbulent potential energy, $b = (g/\rho_0)\overline{\rho w}$ is the buoyancy flux, and $\epsilon_{KE}$, $\epsilon_{PE}$ are the dissipation rates of *KE* and *PE*, respectively. Integrating the energy from $t = 0$ to large times $t \gg L_0/u_0$ yields

$$KE_t - KE_0 = -B - D_{KE} \tag{10}$$

$$PE_t = B - D_{PE} \tag{11}$$

where the subscripts on *KE* and *PE* represent the time at which they are evaluated. For large enough times, $KE_t = PE_t \simeq 0$, from which it follows that $B = D_{PE}$.

There are two irreversible sinks for the turbulence energy, namely the dissipation processes $D_{KE}$ and $D_{PE}$. The $D_{KE}$ process represents the work done against viscous shear stresses at small scales, which increases the internal energy (and the entropy) of the fluid by changing kinetic energy into heat. The $D_{PE}$ process represents the exchange of mass between fluid elements by molecular diffusion and must also be associated with an increase in internal energy (and entropy) of the fluid.

We note that for true homogeneous turbulence, all the averaged properties of the flow, including the buoyancy flux, are uniform. In this idealization, the background mean density field $\overline{\rho(z)}$ is therefore decoupled from the turbulence and remains unchanged. For reasons that will be further explained below, we define a mixing efficiency as $\eta = B/KE_0 = D_{PE}/KE_0$. This mixing efficiency parameter therefore represents the proportion of the total initial energy which, over the duration of the turbulent event, is transferred into potential energy by the generation of a net vertical mass flux through the system (and hence raising the center of gravity of the fluid column).

For the numerical simulations, the turbulence remains homogeneous (but not isotropic) for all times. This includes the buoyancy fluxes and dissipation rates. This implies that in this idealized problem the mean fields are decoupled from the turbulence, so that there is no change in the mean density field and hence no change in the potential energy. For the experiments, the turbulence is homogeneous in the center of the tank, but non-homogeneous near the upper and lower boundaries. In the center of the tank the turbulent density flux is homogeneous, but near the boundaries the gradients of turbulent density flux produce changes to the background mean density profile. These changes in the mean density profile represent an increase in the height of the center of mass of the fluid column and hence an increase in the potential energy. An example of the evolution of the mean vertical density profile in the experiments is shown in Fig. 1.

It may be tempting to conclude from this observation that all the mixing is confined to the regions near the boundaries, but this is not a correct interpretation. Mixing is occurring throughout the tank, but in the homogeneous region away from the boundaries the flux is uniform and divergence free which implies that it does not change the mean density profile. It is only in the non-homogeneous regions near the boundaries that the divergence in the flux (due to the no flux boundary conditions) leads to an accumulation of lighter/heavier fluid at the top/bottom of the tank, which is reflected in the changes to the mean density profile in those regions.

The evolution equation for the total potential energy $E_p$ can be derived from the exact (without making the Boussinesq approximation) continuity equation as

$$\frac{dE_p}{dt} = -\int_S g\rho z\mathbf{u}\cdot\mathbf{n}\,dS + \int_V g\rho w\,dV, \tag{12}$$

in which $V$ is the volume of the fluid, $S$ is the bounding surface of this volume and $\mathbf{n}$ is the unit normal vector pointing outward from $S$. Note that this equation describes the fluxes associated with the turbulent motions only; it does not include the fluxes associated with molecular diffusion of the background mean density field. For the experiments, the velocities normal to $S$ are zero and therefore $dE_p/dt$ is equal to the second integral in (12). Therefore, the increase in the potential energy of the fluid column in the experiments is equal to the time integral of the second integral in (12)– the buoyancy flux – integrated over the volume of the tank. For the simulations, $dE_p/dt$ is zero, and therefore the two integrals in (12) are equal. The flow (which is periodic in these simulations) of potential energy through the boundaries equals volume integral of the buoyancy flux in the body of the fluid in the computational domain. The key to comparing the simulations with the experiments is to use the time-integrated buoyancy flux from the homogeneous simulations to represent the change in potential energy in the experiments. Therefore, in the homogeneous simulations the mixing efficiency $\eta$ is computed as the time integral of the buoyancy flux divided by the change in turbulent kinetic energy over the same time period.

### 3.3. Simulations

The resolution of the simulations were $32^3$, $64^3$ and $128^3$. This allowed for about a factor of four increase in the Reynolds number $Re = u_0L_0/\nu = 100$, 200 and 400, respectively, in which $\nu$ is the kine-

matic viscosity. Most of the simulations reported here were carried out for Prandtl numbers $Pr = 0.5$. Limited investigation of Prandtl number effects were carried out by varying the Prandtl number in the range $0.1 < Pr < 2$. Higher Prandtl numbers could not be achieved without problems in resolving the scalar field: Reynolds numbers were reduced to $Re = 50$ for the $Pr = 2$ cases. Dissipation spectra were used to evaluate resolution issues. These values of $Pr$ are substantially smaller than those for the laboratory experiments.

## 4. Results

There is some arbitrariness in relating the different definitions of the Richardson number used in the laboratory experiments and in the DNS. This relationship could be established using existing grid turbulence data at, say, 10 M downstream from the grid. However, since our interest initially is in the trends of $R_f$ and its maximum magnitude, we will assume that $Ri_b \approx Ri_{t0}$, and we will use the notation $Ri$ to denote the Richardson number given by either of these definitions when we compare the experimental and DNS results. In Section 4.2 we present data for the evolution of the turbulence *activity* parameter $\epsilon/\nu N^2$ for the simulations, which provides a means of linking these results to measurements in the ocean and in the atmosphere. Corresponding results for the grid turbulence experiments are not available since no turbulence measurements were made.

### 4.1. Mixing efficiency

The DNS results for $Pr = 0.5$ are qualitatively consistent with the experimental data, as shown in Fig. 3. For small values of the Richardson number the mixing efficiency increases monotonically, but approaches a constant value of about 30% as the Richardson number increases. The range of Richardson numbers for the DNS is large enough to be conclusive regarding this limit. The asymptotic value of the mixing efficiency in the DNS is about five times larger than the maximum values measured in the experiments. Possible reasons for the large discrepancy between the experimentally measured mixing efficiencies and the DNS results are discussed in the following sections.

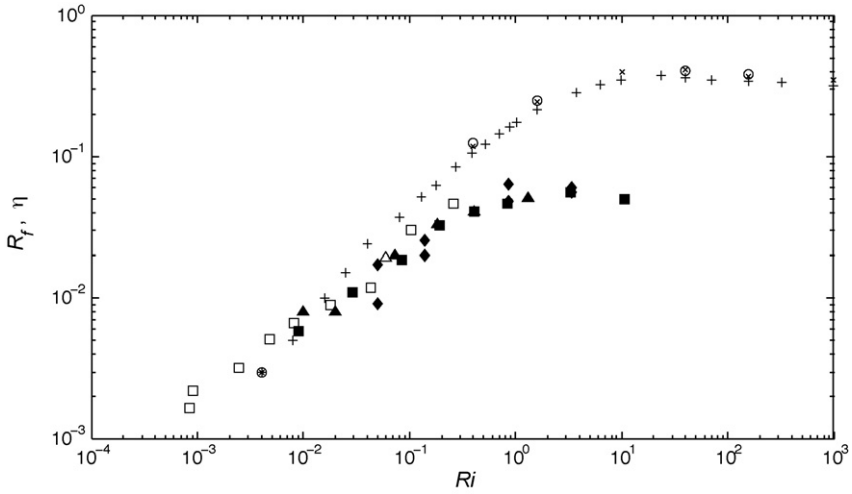


**Fig. 3.** The mixing efficiency plotted versus $Ri$ for both experiments and DNS. (▲) Experimental data from Rottman and Britter (1986), using salt; (■) experimental data from Rehmann and Koseff (2004), using salt; (□) experimental data from Rehmann and Koseff (2004), using heat; (△) experimental data from Rehmann and Koseff (2004), using heat and salt; (♦) experimental data from Britter (1985), using salt; (+) DNS at $32^3$ resolution; (×) DNS at $64^3$ resolution; (○) DNS at $128^3$ resolution.

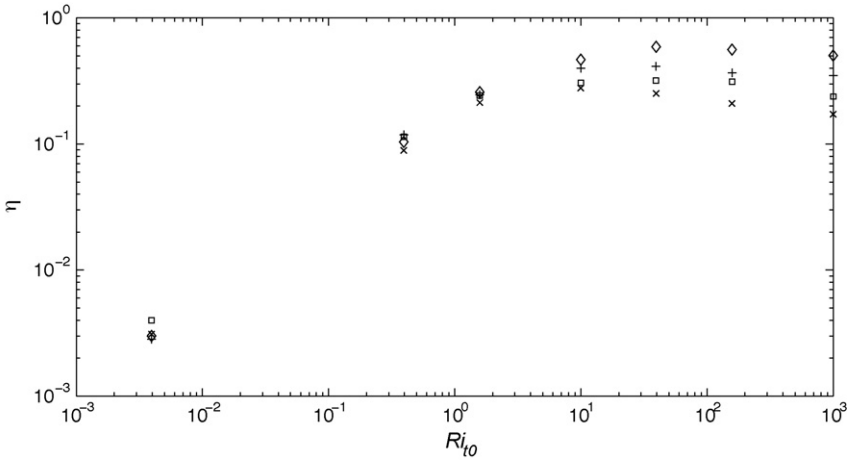


**Fig. 4.** DNS results for mixing efficiency $\eta$ as a function of $Ri_{t0}$ for various values of the Prandtl number $Pr$. (◊) $Pr = 0.1$; (+) $Pr = 0.5$; (□) $Pr = 1.0$; (×) $Pr = 2.0$.

### 4.2. Prandtl number effects

The grid turbulence experiments of Rottman and Britter (1986) and Rehmann and Koseff (2004) cover a range of Prandtl (or Schmidt) numbers $7 < Pr < 700$ using heat and salt stratification. Measurements of the mixing efficiency for different values of the Prandtl number agree to within the experimental uncertainty. Numerical simulations for $0.1 < Pr < 2$ are shown in Fig. 4 and also show only small Prandtl number effects in the regime $Ri_{t0} < 10$. However, simulations of strongly stable cases, $Ri_{t0} > 10$, show that Prandtl number effects increase with stratification. In particular the mixing efficiency decreases with increasing Prandtl number in this regime, a result also reported by Smyth et al. (2001). We note that these molecular effects are likely to be influenced by the relatively low Reynolds (and Peclet) numbers of the simulations. For example Venayagamoorthy and Stretch (2006) have shown that for these DNS simulations, when $Ri_{t0} > 10$, the turbulent mixing is very weak and the diapycnal turbulent diffusivities approach molecular values.

To further elucidate this point and to place these data in the context of measurements in the ocean and atmosphere, the evolution of the parameter $\epsilon/\nu N^2$, which is used in oceanography to measure the activity of the turbulence as described for example in St. Laurent and Schmitt (1999) and Nash and Moum (2002), for the simulations is shown in Fig. 5 for various values of $Ri_{t0}$. Note that Shih et al. (2005) suggest that this parameter may be used to parameterize the turbulent diffusivity in these flows. Fig. 5 shows that for the lower values of $Ri_{t0}$ the turbulence activity parameter starts in the *energetic* or *intermediate* regimes (as defined by Shih et al., 2005) and decay into the *diffusive* regime as the flow evolves. However for the most stable cases ($Ri_{t0} > 10$), the values are within the *diffusive* regime for most of the duration of the simulations. Therefore only weak mixing is present in those cases and molecular effects may be expected to become important. At small dimensionless times, the value of $\epsilon/\nu N^2$ remains nearly constant at a value that decreases with increasing initial turbulence Richardson number, and as the turbulence decays, $\epsilon/\nu N^2$ decreases along a curve that applies for all runs.

Rapid distortion theory (RDT) studies of homogeneous turbulence subject to a uniform stable stratification, have been previously reported by several investigators, e.g. Hunt et al. (1988), Hanazaki and Hunt (1996). These studies have shown how a linear model can accurately reproduce key features of these flows in the strongly stable limit, particularly the vertical buoyancy flux. An example is shown in Fig. 6 where the buoyancy fluxes from DNS and RDT are compared for $Ri_{t0} = 1000$. The RDT result was obtained by simply turning off the non-linear terms in the DNS and therefore has identical initial conditions to the full non-linear simulation. The correspondence clearly indicates that the vertical

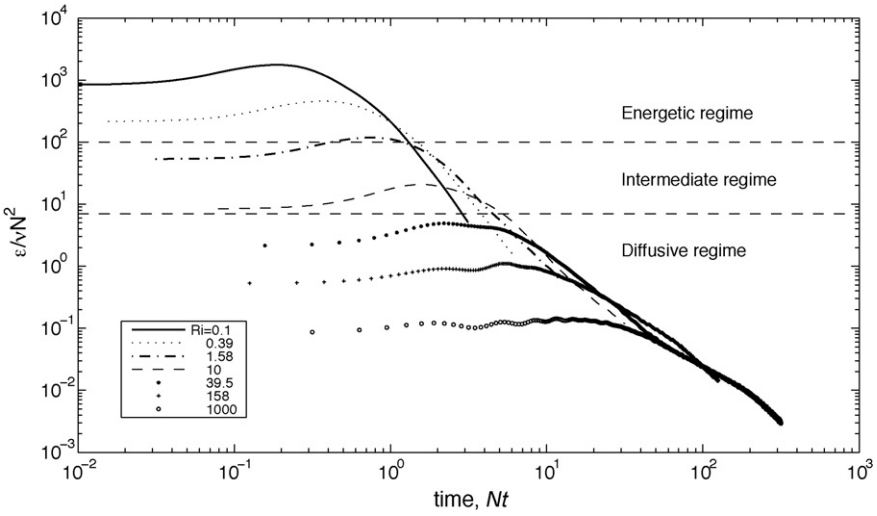


**Fig. 5.** The evolution of the turbulence *activity* parameter $\epsilon/\nu N^2$ as a function of $Nt$. The *energetic*, *intermediate* and *diffusive* regimes are defined in Shih et al. (2005).

dynamics are essentially linear in this strongly stable limit, as discussed further in Venayagamoorthy and Stretch (2006). The small divergence at late times is due to slightly lower dissipation in the linear case.

Since RDT provides a good description of the vertical motion and buoyancy flux for strong stratification we have used it to further explore the issue of Prandtl number effects on mixing efficiency. Results for $Ri = 1000$ are shown in Fig. 7 and suggest that $R_f \sim Pr^{-(1/2)}$ in this strongly stable regime. We note that it can be shown that RDT calculations for the idealized case of an inviscid, non-diffusive fluid, predicts a constant mixing efficiency of 25% for all $Ri_{t0}$. It is evident from the results shown in Fig. 7 that for $Pr \approx 700$ (salt) the mixing efficiency in the strongly stable cases can reduce significantly below those shown in Fig. 4, and may account for some of the difference between the DNS and experimental results. However, since the experiments were all in the regime $Ri_{t0} < 10$ where turbulent mixing is

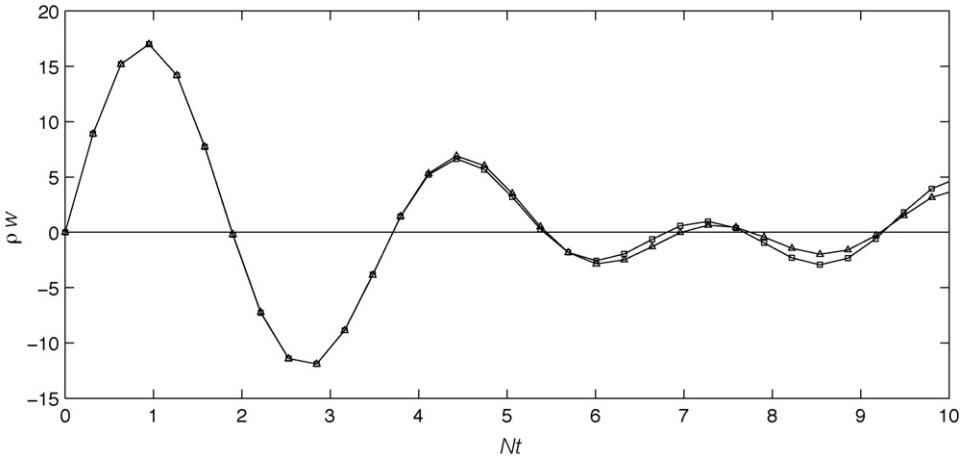


**Fig. 6.** Comparison of the nondimensional buoyancy fluxes from DNS (△) and RDT (□) for $Ri_{t0} = 1000$. In this plot, the buoyancy flux is made nondimensional using the initial velocity scale $u_0$, the length scale $L_0$, and the density scale $L_0|\partial\bar{\rho}/\partial z|$.

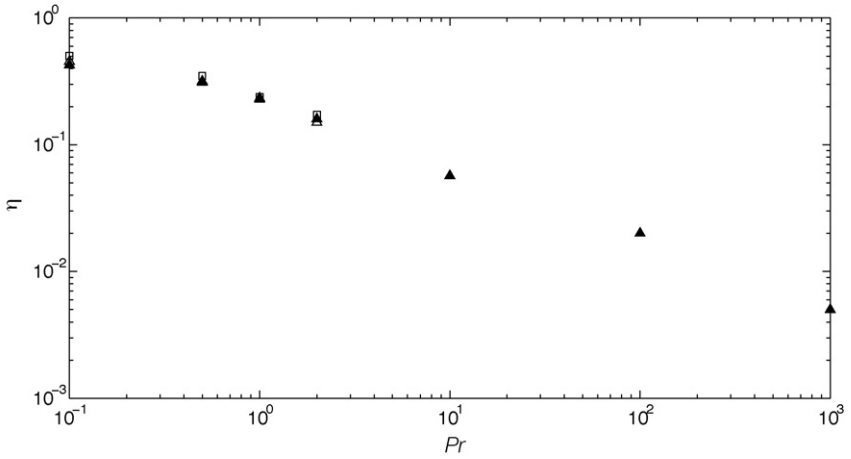


**Fig. 7.** Asymptotic mixing efficiency $\eta$ as a function of Prandtl number $Pr$ for $Ri_{t0} = 1000$. The results for $0.1 < Pr < 2$ are from fully non-linear DNS while those for larger $Ri_{t0}$ are RDT simulations (obtained by neglecting the non-linear terms in the numerical simulations). (▲) RDT ($Re = 100$); (△) DNS ($Re = 100$); (□) DNS ($Re = 200$).

stronger and molecular effects are less important, the issue remains inconclusive. Further investigation of mixing in strongly stable flows at high Reynolds and Peclet numbers is required for a definitive conclusion.

### 4.3. Initial conditions

An alternative explanation for the low mixing efficiencies obtained in the experiments concerns the validity of the assumption that all the work done in towing the grid is transferred into turbulent kinetic energy which is available for mixing the fluid. For example, the possibility that some of this work goes into the excitation of surface waves is ignored despite observations reported by Rottman and Britter (1986) of significant surface disturbances.

The average energy per unit volume, $e_T$, input into the water by towing the grid through it is

$$e_T = C_D \frac{1}{2} \rho_0 U^2. \tag{13}$$

The ratio of the energy input in towing the grid to the turbulent kinetic energy may be expressed as

$$R = \frac{e_T}{(1/2)\rho_0 q_0^2} = C_D \frac{U^2}{q_0^2}, \tag{14}$$

where $q_0^2/2$ is the turbulent kinetic energy just downstream of the grid. In the analysis of the experiments it was assumed that $R = 1$, and since $C_D \simeq 1$, this in turn implies that $q_0/U \simeq 1$. If instead of assuming a value for $R$, we assume that $q_0/U \approx 0.45$, then the experimentally determined mixing efficiencies would be higher by a factor of five, which would agree with the DNS results. Direct turbulence measurements were not made in these experiments but other grid turbulence measurements suggest $q/U \approx 0.1$ at $x/M = 10$. It therefore seems reasonable to conclude that only a fraction of the towing work is actually emerging in the form of turbulent kinetic energy downstream of the grid.

We speculate that small amplitude free-surface or internal standing waves ("sloshing" modes) are initiated by the grid tows and that the energy in these waves can account for the remaining energy. For free-surface waves, linear theory gives an estimate of the energy $E_s$ in the fundamental "sloshing" mode (which has a wavelength equal to twice the length of the tank) as

$$E_s = \frac{1}{4} \rho_0 g a^2 L_T W_T \tag{15}$$

where $a$ is the wave amplitude. As a proportion of the work done in towing the grid, the energy in the sloshing mode may be expressed as

$$\frac{E_s}{E_T} = \frac{1}{2}\frac{1}{C_D}\left(\frac{gH}{U^2}\right)(a/H)^2, \tag{16}$$

where $E_T = e_T H W_T L_T$ is the total work done in towing the grid one length of the tank with water depth $H$. For typical values of $gH/U^2$ used in the experiments, a sloshing amplitude of 5% of the water depth could account for all of the towing work.

For internal waves, linear theory gives an estimate of the energy $E_i$ in the fundamental mode 1 "sloshing" mode (which has a wavelength equal to twice the length of the tank) as

$$E_i = \frac{1}{8}\rho_0 N^2 a^2 H L_T W_T \tag{17}$$

where $a$ is the wave amplitude. As a proportion of the work done in towing the grid, the energy in the fundamental internal sloshing mode may be expressed as

$$\frac{E_I}{E_T} = \frac{1}{4}\frac{1}{C_D}\left(\frac{N^2H^2}{U^2}\right)(a/H)^2. \tag{18}$$

For typical values of $NH/U$ used in the experiments, a sloshing amplitude of 10–20% of the water depth could account for all of the towing work.

## 5. Conclusions

We have used DNS to study mixing efficiency in decaying, homogeneous, stably-stratified turbulence, and have compared the results with grid turbulence experiments. The DNS estimates of mixing efficiency have the same qualitative behaviour with stratification as seen in the experiments. That is, the mixing efficiency increases with stratification for small values of the Richardson number and approaches a constant value at large values. The DNS results confirm the tentative conclusion based on experiments that the mixing efficiency is approximately constant for strong stratification. However, the DNS results for the maximum mixing efficiency ($\sim$ 30%) is much larger than the experimental value ($\sim$ 6%). Constant mixing efficiencies of about 20% are typically assumed for estimates of mixing in the ocean (see, for example, Gregg, 1987), which is predominantly characterized by strong stratification.

Two plausible explanations the lower mixing efficiencies in the experiments have been discussed. First, we have shown that for strong stratifications ($Ri_{t0} \gtrsim 10$) and weak turbulence, the mixing efficiency can be strongly influenced by the Prandtl (or Schmidt) number. The data further suggests that these effects become small for $Ri_{t0} < 10$ where the turbulent mixing is stronger. Prandlt number effects on the mixing efficiency of unstable shear layers were reported by Smyth et al. (2001). Further investigation of mixing in strongly stable flows at higher Reynolds and Peclet numbers is required to produce a definitive conclusion concerning these effects. Our second explanation does not invoke molecular effects but instead concerns the assumption that all the work done in towing the grid is transferred into the turbulent kinetic energy of the fluid. We suggest that a significant portion of the energy may go into the excitation of free surface and internal waves, and show that correction for this effect can significantly increase the experimentally determined mixing efficiencies. This suggestion can be tested experimentally by using a towing tank with a rigid lid to prevent the excitation of surface waves. If our supposition is correct, the drag coefficient of the towed grid should be significantly reduced when a lidded tank is used.

Since the experiments were all in the regime $Ri_b < 10$, we tentatively conclude that $Pr$ number effects are not likely to account for the observed differences in mixing efficiency between the simulations and experiments; therefore, we feel that our second explanation is more probable. However, further investigation of this issue is required.

## Acknowledgment

DDS would like to thank Prof. Jim Riley for providing his DNS code and for many interesting discussions.

## References

Barrett, T.K., Van Atta, C.W., 1991. Experiments on the inhibition of mixing in stably stratified decaying turbulence using laser Doppler anemometry and laser-induced fluorescence. Phys. Fluids A3, 1321–1332.
Barry, M.E., Ivey, G.N., Winters, K.B., Imberger, J., 2001. Measurements of diapycnal diffusivities in stratified fluids. J. Fluid Mech. 442, 267–291.
Britter, R.E., 1985. Diffusion and decay in stably-stratified turbulent flows. In: Hunt, J.C.R. (Ed.), Turbulence and Diffusion in Stable Environments. Claredon, Oxford, pp. 3–13.
Caulfield, C.P., Peltier, W.R., 2000. The anatomy of the mixing transition in homogeneous and stratified free shear layers. J. Fluid Mech. 413, 1–47.
Dewar, W.K., Bingham, R.J., Iverson, R.I., Nowacek, D.P., St. Laurent, L.C., Wiebe, P.H., 2006. Does the marine biosphere mix the ocean? J. Mar. Res. 64, 541–561.
Gregg, M.C., 1987. Diapycnal mixing in the thermocline: a review. J. Geophys. Res. 92, 5249–5286.
Gregg, M.C., 1998. Estimation and geography of diapycnal mixing in the stratified ocean. In: Imberger, J. (Ed.), Physical Processes in Lakes and Oceans, Coastal and Estuarine Studies, vol. 54, American Geophysical Union, Washington, DC, pp. 305–338.
Hanazaki, H., Hunt, J.C.R., 1996. Linear processes in unsteady stably stratified turbulence. J. Fluid Mech. 318, 303–337.
Hunt, J.C.R., Stretch, D.D., Britter, R.E., 1988. Length scales in stably stratified turbulent flows and their use in turbulence models. In: Stably Stratified Flow and Dense Gas Dispersion. Clarendon Press, UK.
Ivey, G.N., Winters, K.B., Koseff, J.R., 2008. Density stratification, turbulence, but how much mixing? Ann. Rev. Fluid Mech. 40, 169–184.
Kaneda, Y., Ishida, T., 2000. Suppression of vertical diffusion in strongly stratified turbulence. J. Fluid Mech. 402, 311–327.
Kimura, Y., Herring, J.R., 1996. Diffusion in stably stratified turbulence. J. Fluid Mech. 328, 253–269.
Linden, P.F., 1979. Mixing in stratified fluids. Geophys. Astrophys. Fluid Dyn. 13, 3–23.
Linden, P.F., 1980. Mixing across a density interface produced by grid turbulence. J. Fluid Mech. 100, 691–703.
Metais, O., Herring, J.R., 1989. Numerical simulations of freely evolving turbulence in stably stratified fluids. J. Fluid Mech. 202, 117–148.
Nash, J.D., Moum, J.N., 2002. Microstructure estimates of turbulent salinity flux and the dissipation spectrum of salinity. J. Phys. Oceanogr. 32, 2312–2333.
Park, Y.G., Whitehead, J.A., Gnanadeskian, A., 1994. Turbulent mixing in stratified fluids, layer formation and energetics. J. Fluid Mech. 279, 279–311.
Rehmann, C.R., Koseff, J.R., 2004. Mean potential energy change in stratified grid turbulence. Dyn. Atmos. Oceans 37, 271–294.
Rehmann, C.R., Koseff, J.R., 2005. Erratum to "Mean potential energy change in stratified grid turbulence" [Dynamics of Atmospheres and Oceans 37 (2004) 271–294]. Dyn. Atmos. Oceans 40, 305–308.
Riley, J.J., Metcalfe, R.W., Weissman, M.A., 1981. Direct numerical simulations of homogeneous turbulence in density-stratified fluids. In: West, B.J. (Ed.), Non-linear Properties of Internal Waves, Proceedings of the AIP Conference. La Jolla Institute.
Rottman, J.W., Britter, R.E., 1986. The mixing efficiency and decay of grid-generated turbulence in stably stratified fluids. In: Proceedings of the 9th Australasian Fluid Mechanics Conference, Univ. of Auckland, December 8–12, 1986, Auckland, New Zealand.
Shih, L.H., Koseff, J.R., Ivey, G.N., Ferziger, J.H., 2005. Parameterization of turbulent fluxes and scales using homogeneous sheared stably stratified turbulence simulations. J. Fluid Mech. 525, 193–214.
Smyth, W.D., Moum, J.N., Caldwell, D.R., 2001. The efficiency of mixing in turbulent patches: inferences from direct simulations and microstructure observations. J. Phys. Oceanogr. 31, 1969–1992.
St. Laurent, L.D., Schmitt, R.W., 1999. The contribution of salt fingers to vertical mixing in the North Atlantic Tracer Release Experiment. J. Phys. Oceanogr. 29, 209–218.
Staquet, C., 2000. Mixing in a stably stratified shear layer: two- and three-dimensional numerical experiments. Fluid Dyn. Res. 27, 367–404.
Staquet, C., Bouruet-Aubertot, P., 2001. Mixing in weakly turbulent stably stratified flows. Dyn. Atmos. Oceans 34, 81–102.
Townsend, A.A., 1976. The Structure of Turbulent Shear Flow. Cambridge University Press.
Venayagamoorthy, S.K., Stretch, D.D., 2006. Lagrangian mixing in decaying stably stratified turbulence. J. Fluid Mech. 564, 197–226.